Materials Science-Poland, Vol. 24, No. 1, 2006

Structure and electrical properties of oxide-ion conductors in the Bi_3NbO_7–Bi_3YO_6 system

A. KOZANECKA-SZMIGIEL[1], F. KROK[1*], I. ABRAHAMS[2**]
W. WROBEL[1], S. C. M. CHAN[2], J. R. DYGAS[1]

[1]Faculty of Physics, Warsaw University of Technology, ul. Koszykowa 75, 00-662, Warsaw, Poland.

[2]Centre for Materials Research, Department of Chemistry, Queen Mary, University of London, Mile End Road, London E1 4NS, United Kingdom

A study of the structure and electrical conductivity of $Bi_3Nb_{1-x}Y_xO_{7-x}$ is presented. X-ray diffraction confirms full solid solution formation ($0.0 \le x \le 1.0$) in this system, with the adoption of a fluorite-type structure. Superlattice ordering of the anion sublattice is evident in neutron diffraction data, the nature of which varies with composition. At low values of x, long-range ordering is present, whereas above $x = 0.4$ only local ordering is observed. Arrhenius plots of the total electrical conductivity of all samples containing yttrium show two linear regions with different activation energies, with evidence for a phase transition between 450 and 680 °C.

Key words: *bismuth oxide; bismuth-niobium-yttrium oxide; oxide-ion conductor; solid electrolyte*

1. Introduction

Solid electrolytes based on δ-Bi_2O_3 show extremely high oxide-ion conductivity and are of interest for electrochemical devices. The high conductivity of δ-Bi_2O_3 originates in its defect cubic fluorite-type crystal structure. The structure is very open and has a high intrinsic vacancy concentration (25%) on the anion sublattice, which along with a high polarizability of Bi $6s^2$ lone pairs results in remarkable oxide ion conductivity. The δ-Bi_2O_3 phase is only stable over a narrow temperature range, namely 730–825 °C [1], which is one of the reasons excluding it from practical application in devices. It was shown that this fluorite-type phase can be stabilized down to room temperature through the formation of a solid solution with other metal oxides

[*]Corresponding author, e-mail: fkrok@mech.pw.edu.pl
[**] Corresponding author, e-mail: I.Abrahams@gmul.ac.uk

[2–7]. This usually leads to a decrease in conductivity at high temperatures, but also to a significant increase in low temperature conductivity (below ca. 600 ^{o}C). For many of the stabilized compounds, the dependence of conductivity on temperature shows an Arrhenius-type behaviour over two distinct temperature regions. These two regions have different activation energies and have been connected to the existence of an ordered phase at low temperatures and a disordered phase at high temperatures.

Several fluorite-related phases have been isolated in the Bi_2O_3–Nb_2O_5 binary system [8–10]. At a 3:1 mole ratio, room temperature stabilization of a fluorite-type structure with a formula of Bi_3NbO_7 is observed [11]. The electrical conductivity of this compound is not particularly high, mainly because of a significantly lower vacancy concentration compared to its parent δ-Bi_2O_3. Using Bi_3NbO_7 as a base composition, however, it is possible to increase the vacancy concentration and therefore conductivity through subvalent substitution of Nb by suitable cations [12]. Substitution by Y^{3+} represents a system, in which a full solid solution might be possible, since Bi_3YO_6, which corresponds to the fully substituted compound, is known to adopt a cubic fluorite-type structure [13]. Here we present an investigation of the structural and electrical effects of yttrium substitution into Bi_3NbO_7, using X-ray and neutron diffraction and AC impedance spectroscopy.

2. Experimental

Preparations. Samples of $Bi_3Nb_{1-x}Y_xO_{7-x}$ ($0.0 \le x \le 1.0$) were prepared using appropriate amounts of Bi_2O_3 (Aldrich, 99.9%), Y_2O_3 (Aldrich, 99.99%), and Nb_2O_5 (Aldrich, 99.9%). Starting mixtures were ground in ethanol using a planetary ball mill. The dried mixtures were heated initially at 740 °C for 24 h, then cooled, reground and pelletised. Pellets were pressed isostatically at the pressure of 400 MPa, then sintered at 800 °C for 10 h. Sintered samples were slowly cooled in air for over 12 h.

Electrical measurements. Electrical parameters were determined by ac impedance spectroscopy up to ca. 800 °C using a fully automated Solartron 1255/1286 system in the frequency range fro 1 Hz to 5×10^5 Hz. Samples for impedance measurements were prepared as rectangular blocks (ca. $6 \times 3 \times 3$ mm^3), cut from slowly cooled sintered pellets using a diamond saw. Platinum electrodes were sputtered by cathodic discharge. Impedance spectra were recorded over two cycles of heating and cooling and collected at programmed temperatures after 15 min of temperature stabilisation. The impedance at each frequency was measured repeatedly until consistency (2% tolerance in drift) was achieved or the maximum number of 25 repeats had been reached.

Crystallography. X-ray powder diffraction data were collected at room temperature on an automated Philips X'Pert X-ray diffractometer using graphite monochromated Cu-K_α radiation (λ_1 = 1.54056 Å and λ_2 = 1.54439 Å). Data were collected in

the flat plate $\theta/2\theta$ geometry in the range of 2θ 10–100°, in steps of 0.02°, with a scan time of 5 s per step.

Powder neutron diffraction data were collected on a Polaris diffractometer at the ISIS facility, Rutherford Appleton Laboratory. Data were collected on back-scattering and low-angle detectors over the respective time of flight ranges of 1.0–20 and 0.5–20 ms. The samples were contained in cylindrical 12 mm vanadium cans located in front of the back-scattering detectors.

3. Results and discussion

X-ray powder diffraction patterns for all studied compositions in the $Bi_3Nb_{1-x}Y_xO_{7-x}$ ($0.0 \le x \le 1.0$) system are presented in Figure 1. It can be seen that basic fluorite structure is maintained throughout the composition range. There is no evidence in the X-ray diffraction patterns for satellite reflections associated with superlattice ordering. Neutron diffraction patterns for the same samples, however, do exhibit additional

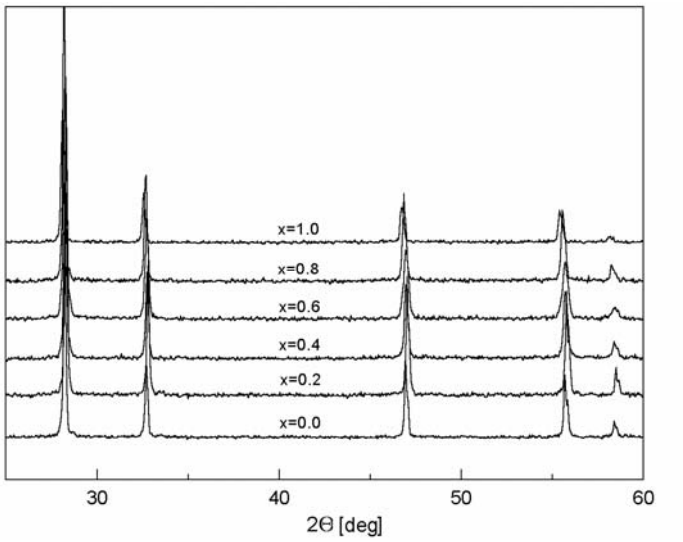

Fig. 1. Room-temperature X-ray diffraction patterns for $Bi_3Nb_{1-x}Y_xO_{7-x}$

peaks (Fig. 2). The presence of these satellite peaks in the neutron diffraction patterns and their absence in the X-ray diffraction patterns suggest that they are due to ordering in the oxide sublattice, which would show weak scattering in X-rays compared to that of heavy cations. The nature of ordering of superlattice changes with composition. At x = 0.0, a large number of weak peaks which could not be indexed on the basic cubic fluorite structure are observed. Ling and Johnson have recently modelled the structure of Bi_3NbO_7 on a tetragonal super cell of dimensions a = 11.52156 Å and

c = 38.5603 Å. [11]. On the substitution of a small amount of Nb by Y this pattern simplifies, but all peaks observed at x = 0.2 are also present in the pattern of the parent compound. At x = 0.4, however, a simpler superlattice structure is detected, with peaks that do not coincide with those observed at lower compositions. At compositions x = 0.6 and x = 0.8 no superlattice peaks are visible, instead a broad hump in the background profile is observed in the range 12–16 ms at the x = 0.6 composition and also to a lesser extent at x = 0.8. The appearance of a broad background feature in the place of superlattice reflections is indicative of a change from long-range vacancy ordering at low substitution levels to local vacancy ordering at higher substitution levels. This local ordering may be interpreted as a random distribution of locally ordered microdomains.

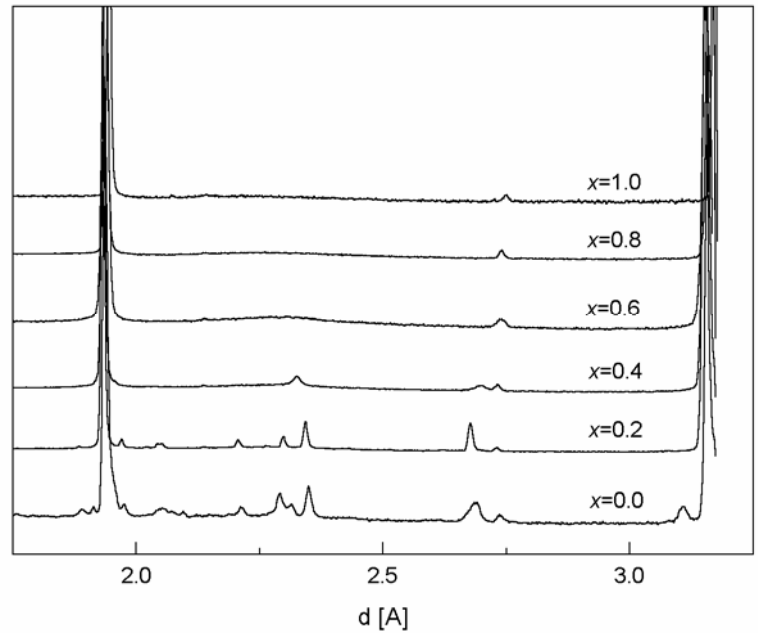

Fig. 2. Room-temperature neutron diffraction patterns for $Bi_3Nb_{1-x}Y_xO_{7-x}$

All samples showed fully reversible conductivity behaviour in heating and cooling runs. The Arrhenius plots of total conductivity during cooling are presented in Figure 3. For x = 0.0, a linear Arrhenius plot is evident over the entire measured temperature range. For all the studied compositions above x = 0.0, two linear regions, one at low and the other at high temperatures, can be distinguished. The appearance of a second linear region at high temperatures probably corresponds to a change in the conduction mechanism, which may be associated with a corresponding phase transition.

Electrical conductivity for compositions with $x \geq 0.4$ shows non-Arrhenius behaviour, with a curvature over a wide range of intermediate temperatures, from 450 to

680 °C. The gradual change in activation energy over a wide temperature range, rather than a sharp transition, is observed in many other systems and may be associated with a kinetically slow change in the favoured conduction mechanism, which may be related to small differences in oxide ion distributions at different temperatures.

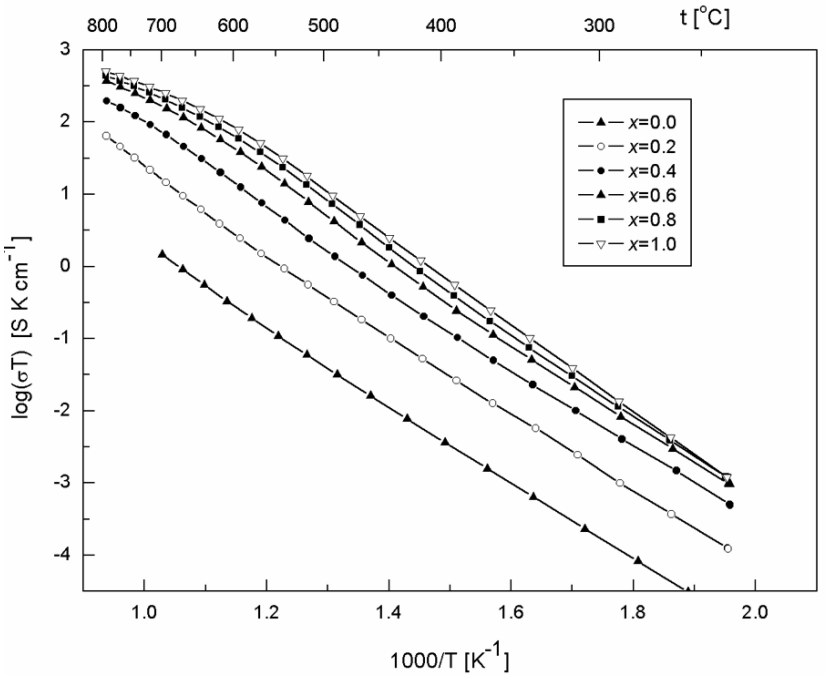

Fig. 3. Arrhenius plots of the total conductivity for various $Bi_3Nb_{1-x}Y_xO_{7-x}$ compositions during first cooling run

The compositional variation of isothermal conductivity at 300 °C (σ_{300}) and the low-temperature conductivity activation energy (ΔE_{lt}) are presented in Figures 4 and 5, respectively. Electrical conductivity exhibits a general increase with increasing yttrium content, which reflects the gradual increase in oxide ion vacancy concentration. Interestingly, the activation energy also shows a general increase with increasing x, from ca. 1.0 eV at x = 0.0 to ca. 1.2 eV at x = 1.0. These phenomena may be explained by considering changes in the defect structure with changing composition. It is clear from the neutron data that there is a change from long-range to short-range ordering in the anion sublattice. Even in the short-range ordered compositions, however, there will still be a significant energy term associated with defect trapping. One must therefore take into account other changes in structure. Indeed, Boyapati et al. [14, 15] have observed a similar behaviour in rare earth-doped bismuth oxide, where both activation energy and conductivity were observed to decrease on ageing, which was attributed to changes in the relative occupancies of normal lattice and interstitial oxide sites. Similar reasoning

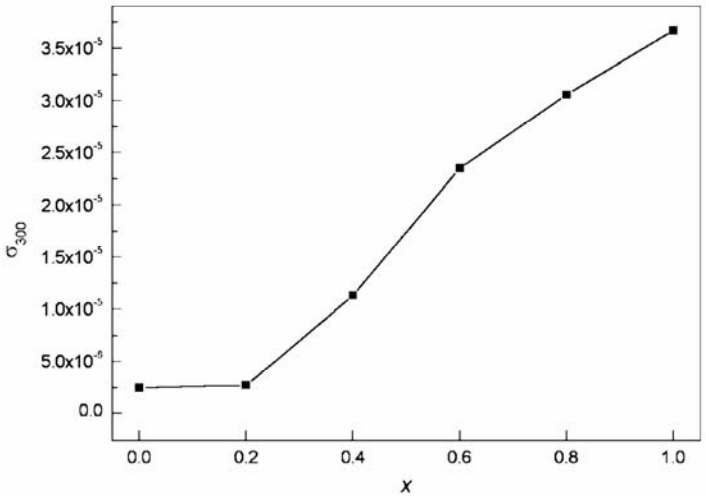

Fig. 4. Compositional variation in total conductivity σ_{300} at 300 ºC for $Bi_3Nb_{1-x}Y_xO_{7-x}$

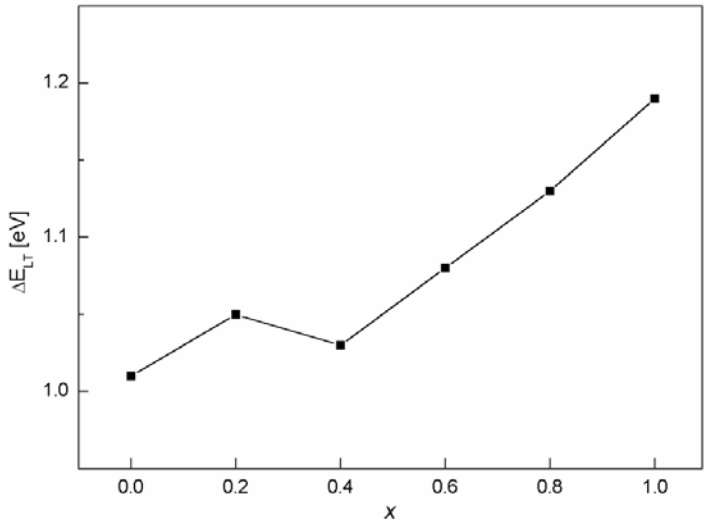

Fig. 5. Compositional variation in low-temperature activation energy ΔE_{lt} for $Bi_3Nb_{1-x}Y_xO_{7-x}$

could be used to explain the observations in the present work, and a detailed analysis of the neutron diffraction data is currently underway.

4. Conclusions

Niobium can be fully substituted by yttrium in Bi_3NbO_7. The obtained solid solution, $Bi_3Nb_{1-x}Y_xO_7$, maintains the basic fluorite-type δ-Bi_2O_3 structure. Long-range superlattice ordering of the anion sublattice was detected in neutron diffraction data at

low levels of substitution, and is replaced by short-range ordering at higher levels of substitution. While changes in the total conductivity reflect an increase in vacancy concentration with increasing yttrium content, the corresponding changes in activation energy are consistent with changes in the distribution of anions within the anion sublattice.

References

[1] TAKAHASHI T., IWAHARA H., NAGAJ Y., J. Appl. Electrochem., 2 (1972), 97.
[2] MAIRESSE G., [in:] *Fast Ion Transport in Solids*, B. Scrosati, A. Magistris, C.M. Mari, G. Mariotto (Eds.), Kluwer, Dordrecht, 1993, p. 271.
[3] BOVIN J.C., MAIRESSE G., Chem. Mater., 10 (1998), 2870.
[4] SHUK P., WIEMHÖFER H.D., GUTH U., GÖPEL W., GREENBLATT M., Solid State Ionics, 89 (1996), 179.
[5] SAMMES N.M., TOMPSETT G.A., NÄFE H., ALDINGER F., J. Eur. Ceram. Soc., 19 (1999), 1801.
[6] AZAD A.M., LAROSE S., AKBAR S.A., J. Mater. Sci., 29 (1994), 4135.
[7] GOODENOUGH J.B., MANTHIRAM A., PARANTHAMAN M., ZHEN Y.S., Mater. Sci. Eng., B12 (1992), 357.
[8] ZHOU W., JEFFERSON D.A., THOMAS J.M., Proc. R. Soc. Lond., A 406 (1986), 173.
[9] LING C.D.,WITHERS R.L., SCHMID S., THOMPSON J.G., J. Solid State Chem., 137 (1988), 42.
[10] CASTRO A., AGUADO E., ROJO J.M., HERRERO P., ENJALBERT R., GALY J., Mater. Res. Bull., 33 (1988), 31.
[11] LING C.D., JOHNSON M., J. Solid State Chem., 177 (2004), 1838.
[12] KROK F., ABRAHAMS I., WROBEL W., CHAN S.C.M., KOZANECKA A., OSSOWSKI T., Solid State Ionics, in press.
[13] BATTLE P.D., CATLOW C.R.A., DRENNAN J., MURRAY A.D., J. Phys C, 16 (1983), 561.
[14] BOYAPATI S., WACHMAN E.D., JIANG N., Solid State Ionics, 140 (2001), 149.
[15] BOYAPATI S., WACHMAN E.D., CHAKOUMAKOS B.C., Solid State Ionics, 138 (2001), 293.

Received 10 December 2004
Revised 10 January 2005